Farshid Sadeghi
Professor
e-mail: sadeghi@ecn.purdue.edu

Behrooz Jalalahmadi
Graduate Research Assistant
e-mail: bjalalah@purdue.edu

Trevor S. Slack
Graduate Research Assistant
e-mail: tslack@purdue.edu

Nihar Raje
Graduate Research Assistant
e-mail: nraje@purdue.edu

School of Mechanical Engineering,
Purdue University,
West Lafayette, IN 47907

Nagaraj K. Arakere
Associate Professor
Mechanical and Aerospace Engineering,
University of Florida,
Gainesville, FL 32611
e-mail: nagaraj@ufl.edu

A Review of Rolling Contact Fatigue

Ball and rolling element bearings are perhaps the most widely used components in industrial machinery. They are used to support load and allow relative motion inherent in the mechanism to take place. Subsurface originated spalling has been recognized as one of the main modes of failure for rolling contact fatigue (RCF) of bearings. In the past few decades a significant number of investigators have attempted to determine the physical mechanisms involved in rolling contact fatigue of bearings and proposed models to predict their fatigue lives. In this paper, some of the most widely used RCF models are reviewed and discussed, and their limitations are addressed. The paper also presents the modeling approaches recently proposed by the authors to develop life models and better understanding of the RCF. [DOI: 10.1115/1.3209132]

Keywords: rolling contact fatigue, bearing life, empirical models, material microstructure

1 Introduction

Ball and roller bearings commonly referred to as bearings are frequently used in simple and complex machinery (e.g., bicycles, gas turbines, transmissions, dental drills, etc.). They are used to allow rotary motion and support significant load. Before the 1940s, their design and application in machinery were more of an art than a science and little was known about their operation. However, since the 1940s, due to ever increasing demand for bearings, usage has required better knowledge and understanding of bearing operation (i.e., elastohydrodynamic lubrication (EHL), dynamics, rolling contact fatigue (RCF), etc.). This paper deals with the bearing rolling contact fatigue empirical and analytical models developed and proposed over the past few decades. It has been proposed that if a ball or a rolling element bearing is properly loaded, lubricated, installed, and kept free of foreign contaminants, then the main mode of failure is material fatigue. Historically, it has also been postulated that a rotating bearing has a limited life because of probability of subsurface initiated fatigue spall. The localized contact stresses in ball and rolling element bearings are extremely high as compared with stresses acting on rotating structural components (e.g., shafts). Neglecting the lubrication effects, stress in bearing contacts is governed by the Hertzian theory, where the pressures are in the order of a few gigapascal. RCF results in metallic particles flaking from the surface of the ball and rolling elements or raceways. When the bearing is properly lubricated this phenomenon commences as a crack below the surface and propagates to the surface causing a pit or a spall in the bearing raceway. The high level of cleanliness of bearing steels in current bearing technology is one factor in minimizing the probability of fatigue spalls [1–5]. A second important factor is the microplastic deformation behavior of bearing steel under the action of RCF. During the running-in process, the bearing raceway material will experience an elastic response after shakedown. The ability to maintain an elastic response during cyclic loading can be compromised by the microstructural changes brought about by microplastic deformation, leading to localized damage and increase in probability for crack initiation and fatigue failure. Physical parameters such as the applied stress level, operating temperature, number of revolutions, and material parameters such as the alloy steel selected, heat treatment, residual stress level, and work-hardening response during running-in affect the ability to maintain an elastic response during cyclic RCF loading. Microplastic deformation precedes crack initiation and typically occurs at microstructural discontinuities such as inclusions and carbide clusters where the resultant stress exceeds the local microyield limit at that fatigue cycle [5]. The cyclic strain amplitudes due to RCF decrease with distance below the running surface [6]. The material degradation due to RCF in ball bearing inner rings can be described as a three-stage process: (I) shakedown, (II) steady-state elastic response, and (III) instability [1–5,7–9]. A residual stress is induced during shakedown with an increase in material strengthening and microyield stress, due to work hardening, and also likely due to the transformation of part of retained austenite to martensite [5,10]. The subsurface volume that is plastically deformed is effectively reduced to nearly zero by over-rolling [5,7]. The length of stage II, where no fatigue damage is thought to occur since cyclic response is elastic [4], is a function of maximum load-induced stress, material characteristics, and operating temperature [10]. The operating temperature is considered to be very significant [5]. Maintaining a stage II elastic response under cyclic loading for as long as possible is critical for extending bearing life, and, hence, understanding the mechanism of stability of stage II can lead to significant improvement in bearing operational reliability. The stability of the finely dispersed carbides in the tempered martensite is thought to be important for extending stage II [5]. Stage III is marked by a decrease in yield stress due to material softening, causing an increase in subsurface volume that is deformed plastically. Carbon diffusion, caused by local temperature peaks, is thought to activate underpinning and poten-

Contributed by the Tribology Division of ASME for publication in the JOURNAL OF TRIBOLOGY. Manuscript received January 6, 2009; final manuscript received July 15, 2009; published online September 24, 2009. Assoc. Editor: Shuangbiao (Jordan) Liu.

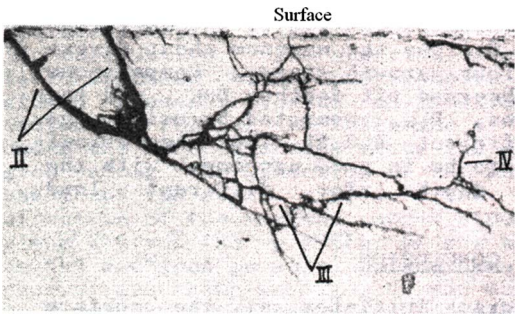

Fig. 1 Subsurface cracks in rolling contact fatigue [14]

tial slip systems, leading to softening. The development of a radial tensile stress and texture development promotes growth of cracks parallel to rolling surface [7,11]. A higher initial load applied during the shakedown stage results in a higher saturation level of work hardening, resulting in extended fatigue life by modifying material response in stages II and III. Apart from rolling element bearings, RCF is also commonly observed in gears, cam-follower mechanisms, and rail-wheel contacts. RCF manifests itself in a variety of different mechanisms that ultimately lead to final failure [12,13]. The two most dominant RCF mechanisms are subsurface originated spalling and surface originated pitting. These are often competing modes of failure, and the ultimate mechanism that prevails depends on a number of factors, e.g., surface quality, lubricant cleanliness, material quality, etc.

Subsurface originated spalling occurs when microcracks originate below the surface at material inhomogeneities such as nonmetallic inclusions and propagate toward the surface to form a surface spall. These cracks are most often found to originate in the region of maximum shear stress below the surface as seen in Fig. 1 (from Ref. [14]). Factors favoring subsurface originated spalling are smooth surfaces, presence of nonmetallic inclusions in the material, and absence of surface shear. This mechanism is the dominant mode of failure in rolling element bearings that have smooth surfaces and operate under EHL conditions. Surface originated pitting, on the other hand, occurs in cases where surface irregularities in the form of dents or scratches are present. Here, cracks initiate at the surface stress concentrators and thereafter propagate at a shallow angle (15–30 deg) to the surface [15]. When they reach a critical length or depth, the cracks branch up toward the free surface, removing a piece of surface material and form a pit as shown in Fig. 2 (from Ref. [16]). This mechanism of failure is common in gears where substantial sliding occurs between the contacting surfaces.

There are a number of differences between classical fatigue and RCF that make it impossible to directly apply the results from classical fatigue to RCF. The most important differences can be listed as follows.

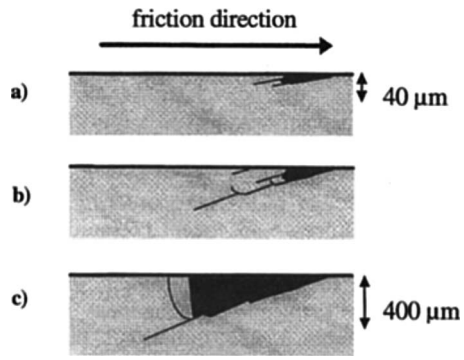

Fig. 2 Mechanism of surface initiated pitting [16]

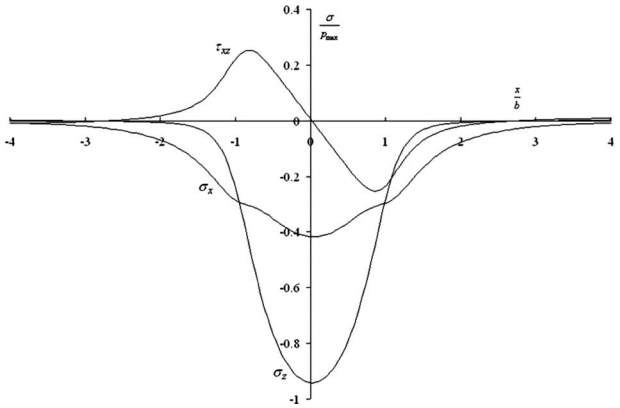

Fig. 3 Stress history at a subsurface point in a Hertzian line contact

1. The state of stress in nonconformal contacts where RCF occurs is complex and multiaxial and governed by the Hertzian contact theory. For the derivation of the subsurface stresses for line and point Hertzian contact, please refer to Refs. [17–24].
2. Contrary to most classical fatigue phenomena, rolling contact fatigue is typically a multiaxial fatigue mechanism. In the past few decades, several multiaxial fatigue criteria have been developed and verified with experiments [25–31].
3. Contrary to classical fatigue, the loading history at a point below the surface is nonproportional; i.e., the stress components do not rise and fall with time in the same proportion to each other; for example, as shown in Fig. 3, the stress history for a point located at the depth where the orthogonal shear stress τ_{xz} is maximum. As seen, there is a complete reversal of the shear stress τ_{xz}, while the normal stresses σ_x and σ_z always remain compressive. Also, the peaks of the two normal stresses do not coincide with the peaks for the shear stress.
4. There is a high hydrostatic stress component present in the case of nonconformal contacts, which is absent in classical tension-compression or bending fatigue.
5. The principal axes in nonconformal contacts constantly change in direction during a stress cycle due to which the planes of maximum shear stress also keep changing. Thus, it is difficult to identify the planes where maximum fatigue damage occurs.
6. The phenomenon of RCF occurs in a very small volume of stressed material, because the contact stress field is highly localized. Typical bearing contact widths are of the order of 200–1000 μm.
7. The evolution of RCF damage leading to a fatigue spall involves a three-stage process: (i) shakedown, (ii) steady-state elastic response, and (iii) instability. Localized plastic deformation and development of residual stresses are precursors to fatigue damage, and therefore the ability to compute the 3D elastic-plastic stress fields that accounts for cyclic loading and traction effects, and acknowledge microstructural changes, is a necessary tool for quantifying raceway fatigue damage.

Since fatigue is the predominant mode of failure in rolling element bearings, the life of bearings is governed by its RCF life. Over the years, several mathematical models have been proposed to estimate lives of bearing components under RCF. These models can be classified into (i) probabilistic engineering models and (ii) deterministic research models. The engineering models are largely empirical in nature and include variables that are obtained from extensive experimental testing. They do not directly consider the details of the constitutive behavior of materials under contact

loading, nor the residual stress and strain computations in the contact areas. The research models, on the other hand, are theoretical in nature, require complete stress-strain behavior information for the materials in contacts, and are used in conjunction with a material failure model. However, these models are usually confined to a specific aspect of the failure process, e.g., only the crack initiation part or only the crack propagation part.

This paper presents a review of existing models for predicting rolling contact fatigue lives for bearings. Sections 2 and 3 provide a review of life models for RCF lives existing in literature. Both analytical and empirical models are discussed and the emphasis is on the models dealing with the subsurface originated spalling. Then, the models developed by the authors for life estimation of the rolling elements are reviewed.

2 Probabilistic Engineering Life Models for Rolling Contact Fatigue

Due to the special nature of RCF and the inability to relate directly to classical component fatigue, most of the early work in determining lives of rolling bearings was based on empirical results and therefore resulting formulas [32]. The first theoretical basis for the formulation of a bearing life model was provided by the seminal work of Lundberg and Palmgren [33,34]. They supposed that a crack initiates a subsurface due to the simultaneous occurrence at a particular depth of the maximum orthogonal shear stress and a weak point in the material. Such weak points were hypothesized to be stochastically distributed in the material. The Weibull statistical strength theory was applied to the stressed volume in a pure Hertzian contact to obtain the probability of survival of the volume from subsurface initiated fatigue. Failure was assumed to be crack initiation dominant. The Lundberg–Palmgren theory [33] states that for bearing rings subjected to N cycles of repeated loading the probability of survival S is given by

$$\ln\frac{1}{S} = A\frac{N^e \tau_0^c V}{z_0^h} \tag{1}$$

where τ_0 is the maximum orthogonal shear stress in the contact, z_0 is the corresponding depth at which this stress occurs, and V is the stressed volume of material. The parameters A, c, and h are material characteristics that are determined experimentally. The parameter e is the Weibull slope for the experimental life data plotted on a Weibull probability paper. The stressed volume of material V was assumed to be

$$V = a\, z_0(2\pi r_r) \tag{2}$$

where the dimensions a, z_0, and r_r correspond to the width, depth, and length of the volume as shown in Fig. 4. The following load-life equation for the bearing was obtained by substituting for τ_0, z_0, and V in terms of the bearing dimensions and contact load in Eq. (1),

$$L_{10} = \left(\frac{C}{P}\right)^p \tag{3}$$

Here, L_{10} is the life for 10% probability of failure, C is the bearing basic dynamic load rating, and P is the equivalent load on the bearing. The exponent p is 3 for ball bearings having an elliptical contact area, 10/3 for roller bearings having modified line contact areas, and 4 for pure line contacts.

Equation (3) formed the basis of the first bearing life standards used in the industry (ISO 281 [35]), and the Lundberg–Palmgren theory [33] has been extensively used since the 1950s. In spite of its wide acceptance, the Lundberg–Palmgren theory [33] suffers from several limitations. It completely overlooks the possibility of surface initiated failure and the presence of a surface lubricating film. The loading on the bearing contact was assumed to be pure normal, with no surface shear traction. However, in practice, some shear traction is always present on the surface, which moves the location of the maximum orthogonal shear stress closer to the surface. Also, the theory assumed the contacting surfaces to be perfectly smooth. In practice, the surfaces contain irregularities such as roughness, scratches, and dents, which deviate the subsurface stress field considerably from a pure Hertzian case.

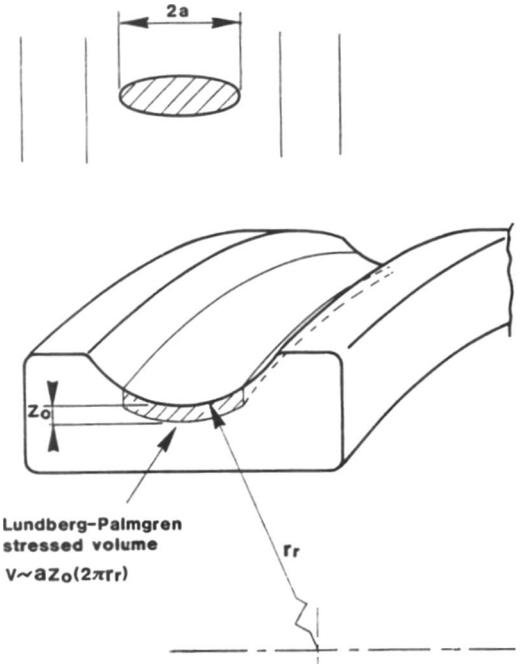

Fig. 4 Stressed volume in the Lundberg–Palmgren theory [33]

Further development in bearing life modeling occurred when Chiu et al. [36] presented a statistical model for subsurface originated spalling in bearing contacts. Spalling was attributed to the presence of material defects having a severity distribution dependent on their size and physical nature. The model was based on a crack propagation law and took into account matrix elastic and plastic properties, defect type, and concentration and geometry of the macrostress field. The model yielded an equation of the following form:

$$\ln\frac{1}{S} = \left(\sum_{i=0}^{4} \phi_i\right) N^\beta \tag{4}$$

where the factors ϕ_i with $i=0-4$ depend on material, geometry, loading, and defect distribution.

Ioannides and Harris [37] proposed a new model for prediction of bearing lives in order to overcome the limitations associated with the Lundberg–Palmgren model [33]. Their model was crack initiation dominated and was based on similar principles as the original Lundberg–Palmgren theory [33] with some modifications. The first distinction was the assumption of discrete material volumes, each with its own probability of survival. The failure risk over each volume was integrated to obtain the overall failure risk for the contact. Second, they recognized the presence of a stress threshold, similar to a fatigue limit for structural components below which no failure was possible. Accordingly, Eq. (1) was modified to

$$\ln\frac{1}{S} = AN^e \int_V \frac{(\sigma - \sigma_u)^c}{z^h} dV, \quad \sigma > \sigma_u \tag{5}$$

where σ is a stress quantity occurring at a depth z, σ_u is the stress threshold, while A is an empirical constant. The stress quantity σ was not limited to the orthogonal shear stress but could be another stress measure, e.g., the maximum shear stress or the equivalent von Mises stress. Then, the load-life equation was correspondingly modified by Ioannides et al. [38] to

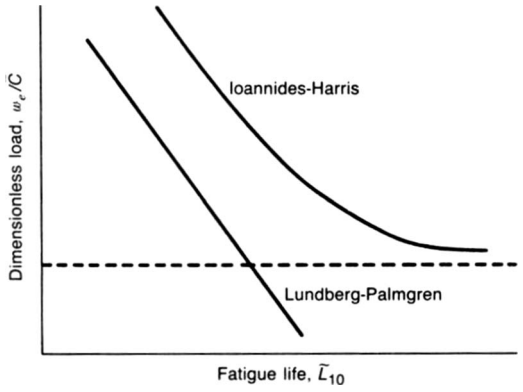

Fig. 5 Comparison between the Lundberg–Palmgren [33] and Ioannides–Harris theories [37]

$$L_{10} = \frac{A}{\left[1 - \left(\frac{P_u}{P}\right)^w\right]^{c/e}} \left(\frac{C}{P}\right)^p, \quad P > P_u \tag{6}$$

where P_u is the load corresponding to the stress threshold σ_u. Figure 5 depicts a comparison between the Lundberg–Palmgren [33] and Ioannides–Harris theories [37]. It is obvious that the Lundberg–Palmgren theory [33] offers a more conservative life estimate. This is mainly because of the greater amount of stressed volume assumed in this theory. Harris and Barnsby [39] developed the Ioannides and Harris [37] method into a more generalized stress-life method. Their method, which was still based on the Lundberg–Palmgren theory, employed a single stress-life factor to modify fatigue life predicted by the Lundberg–Palmgren theory [33]. In the fatigue life prediction for a bearing application, the stress-life factor integrates the effect on life of all applied, induced, and material residual stresses together with empirically determined fatigue limit stresses.

The current ISO standard [35] for rolling bearing life is based on a modification of the Lundberg–Palmgren equation [33] and is given by

$$L = a_1 a_2 a_3 \left(\frac{C}{P}\right)^p \tag{7}$$

where a_1, a_2, and a_3 are life modifying factors that account for reliability, material, and operating conditions.

Schlicht et al. [40] presented a bearing life prediction model based on the following principles: (1) Fatigue failures originate primarily, if not exclusively on the surface; (2) the critical stress leading to failure is the von Mises equivalent stress; and (3) plastic flow and residual stresses that arise in rolling contact cycling are governing factors that influence bearing life. Their life equation was given by

$$L = a_1 a_{23} f_t \left(\frac{C}{P}\right)^p \tag{8}$$

where a_1 is the ISO factor for reliability ($a_1=1$ for $S=0.9$), a_{23} adjusts for operating conditions, and f_t adjusts for the loss of hardness of AISI 52100 steel at higher operating temperatures.

Tallian [41,42] proposed a statistical model for fatigue lives of rolling element bearings based on a given defect severity distribution. The model used the orthogonal shear stress field as a function of depth below the bearing raceway and computed fatigue life as the crack propagation life through this stress field according to a Paris type law. Crack initiation life was assumed to be negligible. The model considered material fatigue susceptibility, fatigue limiting stress, and defect severity distribution as the main parameters. The life equation is given by

$$\ln\frac{1}{S} = \phi_0 \phi_2 \left[\frac{p_{\max}^{\zeta}}{n_0 z_0}\right]^{\beta} N^{\beta} V \tag{9}$$

Here, ϕ_0 is a fatigue susceptibility parameter, ϕ_2 is a defect parameter that takes into account the defect density and severity distribution, n_0 is a dimensionless crack growth integral parameter, z_0 is the depth of occurrence of the maximum orthogonal shear stress, β is the dispersion coefficient, and $\xi=9.4$ is the Paris-law exponent used in the model.

It needs to be pointed out that for a given probability of survival S and given bearing dimensions, the Lundberg–Palmgren equation (Eq. (1)) [33] relates the critical stress-life exponent to the Weibull slope e according to

$$N \propto \frac{1}{\tau_0^{((c-h+1)/e)}} \tag{10}$$

Thus the stress-life exponent depends on the dispersion in bearing life data. However, exponents published in literature appear to be independent of the life dispersion. In recognition of this fact, Zaretsky [43] presented a similar model to Lundberg and Palmgren [33] with two modifications: (1) Dependence of the stress-life relation on the Weibull slope e was eliminated, and (2) dependence on the depth term was eliminated. In addition, the critical stress quantity used was the maximum shear stress instead of the orthogonal shear stress. Zaretsky's equation [43] is given by

$$\ln\tfrac{1}{S} = N^e \tau^{ce} V \tag{11}$$

Harris and McCool [44] carried out a statistical comparison of bearing lives obtained using the Lundberg–Palmgren [33] and Ioannides–Harris [37] theories. For both theories, ratios between predicted lives according to the equations and actual lives observed experimentally were largely distributed.

Kudish and Burris [45] presented a similar model to Tallian [42] for statistical bearing life prediction. Their model included the following parameters: (1) contact pressure and size of contact; (2) friction coefficient; (3) residual stress distribution with depth; (4) initial statistical defect distribution versus defect size, location, and orientation; (5) material fracture toughness; (6) variation of material hardness with depth; and (7) material fatigue parameters as functions of material hardness. The model considers crack propagation from initial cracks as the mechanism of failure and neglects the crack nucleation life. The life in terms of number of cycles N that a contact can withstand with a given survival probability is given by

$$N = \frac{C}{g_0 p_{\max}^n} \tag{12}$$

Here, C is a constant that depends on material fracture toughness while g_0 and n are Paris-law parameters.

Shao et al. [46] and, consequently, Leng et al. [47] recorded the process of development of contact fatigue cracks in a case-hardened steel by tracing crack propagation drawings. They showed that spalling of a case-hardened steel was resulted from the coordinated development of a so-called leading group of cracks, which consists of three to seven cracks. The process of contact fatigue was divided into three stages: the incubation, the stable propagation, and the branching propagation periods. Leng et al. [47] obtained 13%, 56%, and 31% contributions to the fatigue life for these three stages, respectively. They used the dislocation theory to explain the initiation of contact fatigue cracks and concluded that the contact fatigue cracks initiate where the maximum value of $\tau_{\max}$ occurs.

Otsuka et al. [48] developed a test method to obtain the intrinsic mode II crack growth characteristics of metals and suggested, according to their results, that the subsurface cracks due to rolling contact fatigue are produced through the mechanism of mode II fatigue crack growth created by the shear stress component of the contact stress. Miyashita et al. [49] studied the spalling mode of

failure under rolling contact fatigue of sintered alloys using the rolling contact fatigue tests and finite element model (FEM) analysis. The location of the $\Delta\tau_{xy}$ estimated by their FEM analysis coincided with the depth of the crack initiation point observed in their experiment. Similarly, Otsuka et al. [48] showed that subsurface crack growth behavior was controlled by the stress intensity factor range Δk_{II}. Also, they concluded considering the surface friction force causes the depth of maximum shear stress becomes closer to the contact surface. However, the effect of friction force on the value of $\Delta\tau_{xy}$ was not significant.

Shimizu [50] showed that bearing steel does not show any fatigue limit, whereas structural steel does have a distinct fatigue limit. In the absence of a fatigue limit for bearing steel, a third parameter γ known as minimum life prior to failure was proposed for the analysis of fatigue life behavior under a given rolling contact fatigue load, leading to a three-parameter Weibull life distribution function

$$L-\gamma=\left(\frac{C}{F}\right)^{p}\left(\frac{\ln R}{\ln 0.9}\right)^{1/m} \tag{13}$$

where C is dynamic load capacity, F is equivalent load, p is load-life component, R is the survival probability of the inner and outer rings of bearings, m is Weibull slope, and L is fatigue life. Applying the three-parameter Weibull distribution with a normalized Weibull slope $m=10/9$ used in the analysis of a point contact fatigue test data for rotary and linear ball bearings, he calculated a constant value of the load-life exponent $p=8/3$ for both L_{10} and L_{50} lives.

Kotzalas [51] investigated the statistical distribution of tapered roller bearing fatigue lives at high levels of reliability. He showed that the original two-parameter Weibull distribution cannot predict a finite life value for which 100% of the population will survive. However, since empirical evidence of a minimum life at 100% reliability has been shown for through hardened ball and spherical roller bearings, linear ball bearings, and tapered roller bearings, he showed that analytical methods using the three-parameter Weibull distribution are able to detect a finite life at high reliability fatigue.

A concise summary of probabilistic engineering bearing life model development is provided in Table 1, in chronological order, starting with Palmgren's [32] seminal work in 1945 to current models. Since the engineering models are empirical in nature, they offer no significant insights into the physical mechanisms of RCF. On the other hand, the research models are more insightful in this regard and are attempts to explain some of the mechanisms observed during the failure process. Section 3 provides a summary of the research models for estimating the fatigue life of the rolling elements.

3 Deterministic Research Life Models for Rolling Contact Fatigue

The deterministic research models are based on physical principles and take into account the actual mechanics of the failure process. Two different sets of models have been traditionally developed to estimate the fatigue lives: (1) models based on the crack initiation and (2) models based on the crack propagation. However, some models account for both the initiation and propagation parts of life.

The first analytical approach to study the RCF problem was adopted by Keer and Bryant [52] who used two-dimensional fracture mechanics to evaluate fatigue lives for rolling/sliding Hertzian contacts. Their approach assumed the crack initiation life to be small in comparison to the crack propagation life. The number of cycles to failure N was expressed in terms of the maximum Hertzian pressure p_{max} and the contact half-width b as

$$N=\frac{b^{1-m/2}}{\beta_0 p_{\max}^{m}} \tag{14}$$

Here, β_0 and m are material parameters governing the crack growth rate. However, it was found that the fatigue lives calculated using this model were orders of magnitude shorter than those predicted for similar Hertzian pressure using engineering models [41].

Zhou et al. [53,54] introduced a life model that included both the crack initiation and crack propagation lives. The total life was expressed as

$$N=\frac{AW_c}{(\Delta\sigma-2\sigma_k)^2 D}+\int_{a_i}^{a_f}\frac{da}{c\Delta K^n} \tag{15}$$

where A, c, and n are material parameters; W_c is the specific fracture energy per unit area; $\Delta\sigma$ is the local shear stress range; σ_k is the friction stress for the material; D is the damage accumulation factor; and ΔK is the stress intensity factor range at the crack tip.

Bhargava et al. [55] presented a life model based on plastic strain accumulation in strain hardening materials under cyclic contact stress. The spalling lives were predicted from the plastic strain. Cheng and co-workers [56,57] proposed a micromechanical model based on the dislocation pileup theory to estimate the crack initiation life in contact fatigue. Microcracks were assumed to be nucleated in slip bands located in material grains. The microcrack initiation life N_i was given by

$$N_i=\frac{c}{(\Delta\tau-2\tau_f)D} \tag{16}$$

where c is a material constant, $\Delta\tau$ is the critical shear stress amplitude resolved on the slip layer, τ_f is a threshold stress below, which cracks do not initiate, and D is a damage accumulation factor.

Vincent et al. [58] proposed a similar model for crack initiation based on the dislocation pileup idea. Their model took into account the effect of all stress components and also included residual stress effects. Dislocation emissions were assumed to occur due to the presence of subsurface inclusions in the bearing steel matrix that leads to local stress concentrations and local plastic straining. Inclusions were assumed to be spherical. The number of cycles to crack initiation N was found according to the following equation:

$$\frac{\mu}{\pi(1-\nu)}(\gamma_{\rm pl}+2fN\gamma_{\rm pc})\frac{d}{2\lambda}\ln\left[\frac{1}{8}\left\{(\gamma_{\rm pl}+2fN\gamma_{\rm pc})\frac{d}{b'}\right\}^2\right]-\frac{\sigma_x+\sigma_y}{2}=\frac{\mu}{\alpha} \tag{17}$$

Here, μ and ν are the shear moduli and Poisson's ratio for the matrix, f is a damage efficiency accumulation factor, d is the inclusion diameter, λ is the length of the domain in which dislocations are accumulated, $\gamma_{\rm pl}$ is the effective plastic strain after the first loading cycle, $\gamma_{\rm pc}$ is the effective plastic cyclic strain, b' is the modulus of Burgers' vector, σ_x and σ_y are components of the stress tensor, which include the Hertzian as well as residual stresses, and α is the theoretical strength factor of the order of 5 for most metals. Xu and Sadeghi [59] developed an analytical model to investigate the effects of dent on spall initiation and propagation in lubricated contacts. Their model was based on the damage mechanics concept that the fatigue spall initiation and propagation is due to the accumulated plastic strain process rather than the stress intensity at the tip of the crack.

Lormand et al. [60] extended the model of Vincent et al. [58] to include crack propagation according to a Paris law. Crack growth was assumed to occur due to shear stresses (mode II propagation).

Table 1 A chronological listing of probabilistic engineering bearing life prediction model development

Year	Researchers	Ref.	Model description/hypothesis
1945	Palmgren	[32]	Empirical.
1947	Lundberg and Palmgren	[33]	First probabilistic bearing life model, termed the LP model, based on probability of crack initiation at a subsurface depth (z_0) where orthogonal shear stress (τ_0) is maximum in stressed volume (V) in the contact, expresses the probability of survival (S) after N RCF cycles as (Eq. (1)): $\ln(1/S)=A(N^e\tau_0^c V/z_0^h)$, where A, c, and h are experimentally determined material parameters and e is the Weibull slope for the experimental life data.
1952	Lundberg and Palmgren	[34]	The L_{10} life (Eq. (3)) is expressed as $L_{10}=(C/P)^p$, where C is the bearing basic dynamic load rating, P is the equivalent load acting on the bearing, and exponent p depends on contact shape.
1971	Chiu et al.	[36]	Probabilistic model (Eq. (4)) that attributes spalling to intrinsic material defects and includes influence of material elastic and plastic properties, defect type, concentration, and geometry on the contact stress field via factors ϕ_i, given by $\ln(1/S)=(\sum_{i=0}^{4}\phi_i)N^\beta$. β=dispersion coefficient.
1985	Ioannides and Harris	[37]	Improves on the LP model by (i) assuming discrete material volumes, each with its own probability of survival, and overall risk obtained by integration; and (ii) introducing a stress threshold (σ_u) below which no failure is possible, resulting in the following relation (Eq. (5)): $\ln(1/S)=AN^e\int_V \frac{(\sigma-\sigma_u)^c}{z^h}dV, \quad \sigma>\sigma_u.$
1986	Schlicht et al.	[40]	Model assumes that fatigue failures originate at the surface due to von Mises stress, and plastic flow and residual stress development due to RCF influence bearing life. The life model is given by $L=a_1a_{23}f_t(C/P)^p$ where a_1 and a_{23} are life modifying factors based on reliability, material, and operating conditions.
1987	Shao et al.	[46]	The development of cracks due to RCF in case-hardened bearing steels was described by a three-stage process: incubation, stable propagation, and branching/propagation.
1988	Leng et al.	[47]	The three stages described in Ref. [46] were allocated 13%, 56% and 31% contributions to life.
1989	Current ISO Standard	[35]	The life relation is given by $L=a_1a_2a_3(C/P)^p$, where a_i are life modifying factors.
1992	Tallian	41 and 42	Probabilistic life model uses orthogonal shear stress field solution in conjunction with a Paris-law exponent (ζ) and growth parameters (n_0), material fatigue susceptibility (ϕ_0), and defect (ϕ_2) parameters, given by (Eq. (9)): $\ln(1/S)=\phi_0\phi_2[p_{\max}^\zeta/n_0z_0]^\beta N^\beta V$.
1994	Zaretsky	[43]	Life equation (Eq. (11)) is $\ln(1/S)=N^e\tau^{ce}V$ and is similar to LP model, with two modifications: (i) dependence of the stress-life relation on the Weibull slope e was eliminated, and (ii) dependence on the depth term was eliminated. τ^{ce} is the maximum shear stress and not orthogonal shear stress.
1996	Harris and McCool	[44]	Statistical comparison of actual and computed bearing lives from LP and Ioannides and Harris's [37] models showed wide dispersion.
1996	Otsuka et al.	[48]	RCF testing and FEA showed that subsurface crack growth behavior was controlled by mode II stress intensity range, ΔK_{II}.
1999	Ioannides et al.	[38]	The load-life relation, incorporating model in Ref. [37], is given by Eq. (6) as $L_{10}=\left(A/\left[1-\left(\frac{P_u}{P}\right)^w\right]^{c/e}\right)\left(\frac{C}{P}\right)^p, \quad P>P_u,$ where P_u is the load corresponding to σ_u.
2000	Kudish and Burris	[45]	Model improved by Tallian [41,42] by including the effects of contact pressure and size, friction coefficient, residual stresses, initial defect, size, location and orientation distributions, material fracture toughness, material hardness variation with depth, and material fatigue parameters as function of hardness.

Table 1 (***Continued.***)

Year	Researchers	Ref.	Model description/hypothesis
2002	Shimizu	[50]	A three-parameter Weibull life distribution function was proposed, after showing that bearing steels subject to RCF do not exhibit a fatigue endurance limit, given by (Eq. (13)) $L-\gamma=(C/F)^p(\ln R/\ln 0.9)^{1/m}$, where γ is the minimum life prior to failure.
2003	Miyashita et al.	[49]	The location of $\Delta\tau_{xy}$ estimated by FEA was shown to coincide with the depth of crack initiation observed in RCF experiments using sintered alloys.
2005	Kotzalas	[51]	A three-parameter Weibull distribution was shown to be able to predict finite life in the high reliability regime, based on statistical distribution of tapered roller bearings.

However, in order to account for the compressive stress component σ_n acting along the crack faces, a Coulomb friction stress [61] given by

$$\tau_{\text{eff}} = |\tau - c\sigma_n| \tag{18}$$

was assumed. A coefficient of friction $c=0.4$ (used also by Melander [62]) was chosen although no justification for this value was provided. Later, Lormand et al. [63] applied a new physically based model to determine the influence of inclusion population and loading conditions on the distribution of rolling bearing lives. Recently, in order to estimate the rolling contact fatigue range and quality control of bearing steel, Girodin et al. [64] did a statistical analysis of nonmetallic inclusions.

Harris and Yu [65] showed that application of surface shear stresses in combination with Hertz stresses can significantly influence the subsurface octahedral shear stress distribution. However, they concluded that such surface shear stresses do not alter the maximum range of the subsurface orthogonal shear stress. Therefore they suggested using the octahedral shear stress (von Mises stress) as the failure-causing stress in fatigue life prediction analyses.

Jiang and Sehitoglu [66] applied an elastoplastic finite element model that included the effects of cyclic ratcheting in conjunction with a multiaxial fatigue criterion [67] to compute the total life under rolling line contacts. Total damage D was assumed to be a sum of damage due to fatigue D_f and due to ratcheting D_r. Failure was assumed to occur when the total damage equaled unity. This approach was again based only on the crack initiation life and neglected the crack propagation aspect. The rates of damage accumulation for the two phenomena were given by

$$\frac{dD_f}{dN} = \frac{(\text{FP} - \text{FP}_0)^m}{C}, \quad \frac{dD_r}{dN} = \frac{\left|\frac{d\gamma_r}{dN}\right|}{\gamma_{\text{crict}}} \tag{19}$$

where FP is a fatigue parameter; γ_r is the ratcheting strain FP_0; and m, C, and γ_{crict} are material constants. The fatigue parameter FP was related to stresses and strains on a critical plane according to the following multiaxial fatigue criterion [67]:

$$\text{FP} = \frac{\Delta\varepsilon}{2}\sigma_{\max} + J\Delta\gamma\Delta\tau \tag{20}$$

where $\Delta\varepsilon$ is the normal strain range, $\sigma_{\max}$ is the maximum normal stress, $\Delta\gamma$ is the shear strain range, $\Delta\tau$ is the shear stress range, and J is a material dependent constant. They concluded that the combination of fatigue and ratcheting damage is maximum at a depth corresponding to the occurrence of maximum orthogonal shear stress range. This is in accordance with the Lundberg–Palmgren theory [33]. Ringsberg [68] combined elastic-plastic finite element analyses, multiaxial fatigue crack initiation model [67] used together with the critical plane concept, fatigue damage summation calculations, and comparison of results from numerical analyses and experiments to develop a strategy for fatigue life prediction of rolling contact fatigue crack initiation. He concluded that the strategy developed has the capacity to predict the position for greatest fatigue damage, the orientation of crack planes, and the fatigue life to crack initiation due to both low-cycle fatigue and ratcheting. Multiaxial fatigue damage due to RCF using the critical plane approach, with applications to railway wheel contact fatigue, is addressed by Liu et al. [69] and Liu and Mahadevan [70]. Table 2 provides a concise summary of the deterministic models, in chronological order.

4 Limitations of Existing Life Models

The research models proposed in literature are based on a homogeneous description of material in the contact region to estimate the contact fatigue life. Such homogeneous material description overlooks the inhomogeneities such as nonmetallic inclusions that are invariably present in the contact region as byproducts of the bearing manufacturing methods, as shown, for example, in Fig. 6 (from Ref. [71]). These inclusions often act as nucleation sites for the fatigue cracks [72,73]. The inclusions not only cause early damage due to their inferior strength properties but also cause local stress concentrations owing to their differential constitutive properties in relation to the surrounding matrix [74,75]. In addition, nonmetallic inclusions cause stress induced microstructural alterations in the surrounding matrix under cyclic loading [76,77]. These structural changes assist in the fatigue process. Two commonly structural changes occurring under the raceway in rolling element bearings are the "butterfly" effect as shown in Fig. 7 (from Refs. [78,79]), and slip bands as shown in Fig. 8 (from Ref. [79]).

Very few models relate the micromechanical material behavior to the phenomenon of RCF. The first fatigue cracks invariably appear as microcracks at weak material points, and the crack initiation mechanism is influenced by the microscopic characteristics of the material. Therefore, the models that are based on a macroscale description of the material tend to overlook the microscopic details. Rolling contact fatigue lives of bearings are known to show scatter because of the spatial dispersion in material strengths and inclusion distributions. In fact, experimentally observed bearing lives follow the Weibull distribution closely. The process of crack initiation is essentially one of seeking the weakest point in the material where the local strength is a minimum. However, the analytical models proposed in literature are deterministic in nature and hence do not take this into account. Also, from experimental evidence, the material properties under contact fatigue are nonuniform but vary along different subsurface layers [56]. This is another aspect that is overlooked in previous analytical models.

On the other hand, in the engineering life models, different critical stress criteria have been proposed to be used in the life equation. These include the orthogonal shear stress [33], the maximum shear stress [80], the von Mises stress [37], and the octahedral shear stress [54]. Note that the maximum value of each stress measure occurs at different depths below the surface in a bearing

Table 2 A chronological listing of deterministic research bearing life prediction model development

Year	Researchers	Ref.	Model description/hypothesis
1983	Keer and Bryant	[52]	First deterministic analysis of RCF life. A 2D fracture mechanics approach is used for life estimation in rolling/sliding Hertzian cylindrical contacts assuming initiation life is small compared with propagation life. Cycles to failure $N=b^{1-m/2}/\beta_0 p_{\max}^m$, where $p_{\max}$ is maximum Hertz pressure, b is contact half-width, and β_0 and m are crack growth parameters. Life computed greatly underpredicted compared with LP-based models.
1989	Zhou et al.	[53]	Model included both crack initiation and propagation lives. The total life is (Eq. (15)) $N=AW_c/(\Delta\sigma-2\sigma_k)^2D+\int_{a_i}^{a_f}(da/c\Delta K^n)$, where A, c, and n are material parameters; σ_k is the specific fracture energy per unit area; W_c is material friction stress; D is the damage accumulation factor; and ΔK is the stress intensity factor range at the crack tip.
1990	Bhargava et al.	[55]	Model based on plastic strain accumulation in strain hardening materials under cyclic RCF.
1992	Sehitoglu and Jiang	[67]	Multiaxial fatigue crack initiation model for RCF.
1993	Zhou	[54]	Extension to model in Ref. [53].
1994	Cheng et al.	[56]	Micromechanical model based on dislocation dynamics (pileup). Crack nucleation was assumed to take place in slip bands at the grain level. Initiation life is given by (Eq. (16)) $(N_i=(c/(\Delta\tau-2\tau_f)D)$, where $\Delta\tau$ is the critical shear stress amplitude and τ_f is a threshold.
1995	Cheng and Cheng	[57]	
1997	Melander	[62]	A FEA study of cracks subjected to RCF including crack face friction due to closure.
1998	Vincent et al.	[58]	Crack initiation model based on dislocation pileup and accounted for full stress tensor and residual stress field. Dislocation emissions were assumed to occur due to the presence of subsurface inclusions that lead to stress concentration and localized slip/plasticity.
1998	Lormand et al.	[60]	Extension of model in Ref. [58] to include crack propagation via Paris law, driven by mode II loading. A Coulomb stress was included to account for crack face friction due to closure.
1999	Harris and Yu	[65]	The inclusion of surface traction along with Hertzian normal pressure was shown to significantly increase subsurface octahedral shear stress (von Mises stress), but not the maximum stress range.
1999	Jiang and Sehitoglu	[66]	Elastic-plastic FEA that included effects of ratcheting under RCF in conjunction with a multiaxial fatigue damage criterion was used to compute initiation life for line contacts (Eqs. (19) and (20)). Maximum damage corresponded to depth where orthogonal shear stress range was maximum, in accordance with LP theory.
2001	Ringsberg	[68]	Elastic-plastic FEA, multiaxial fatigue crack initiation model based on a critical plane approach, and fatigue damage accumulation concepts were used to develop a procedure for life prediction under RCF loading.
2006	Liu et al.	[69]	Multiaxial fatigue damage due to RCF using the critical plane approach, with applications to railway wheel contact fatigue.
2007	Liu and Mahadevan	[70]	A unified multiaxial fatigue damage model for RCF using the critical plane approach for isotropic and anisotropic materials.

contact and is different in magnitude. Hence, each criterion predicts a different depth where crack initiation could occur. Experimentally, cracks have been found to initiate at various depths below the contact surface [81–83]. Therefore, the exact stress measure governing crack initiation under rolling contact conditions is not clear yet. Moreover, calibration of the engineering life models requires extensive RCF endurance testing that becomes both expensive and time consuming. From a practical point of view, a model with a few input parameters that can be calibrated easily using simple and inexpensive bench tests is desired.

In view of the limitations of the current state of bearing life modeling, some modeling approaches, for predicting the fatigue lives of the rolling element bearings, recently proposed by the authors are summarized in Sec. 5. The new approaches investigate

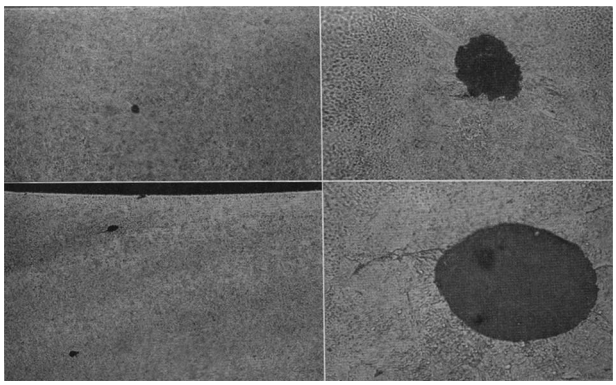

Fig. 6 Subsurface inclusions in bearing steel AISI-52100 [71]

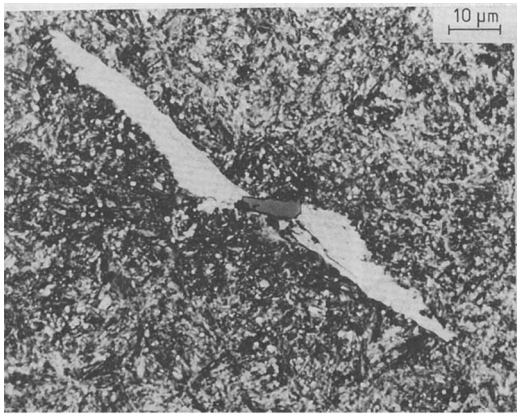

(*a*)

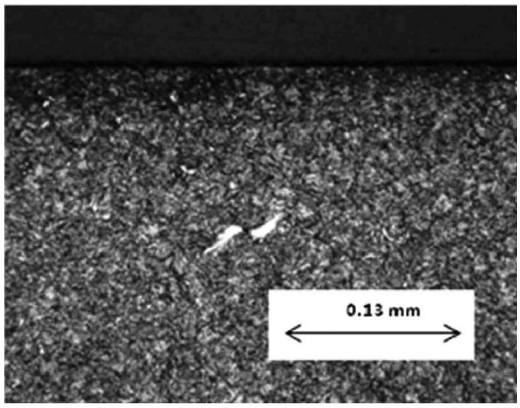

(*b*)

Fig. 7 Formation of butterflies around nonmetallic inclusion under rolling contact: (*a*) bearing steel AISI-52100 [78], and (*b*) bearing steel M50 074A [79]

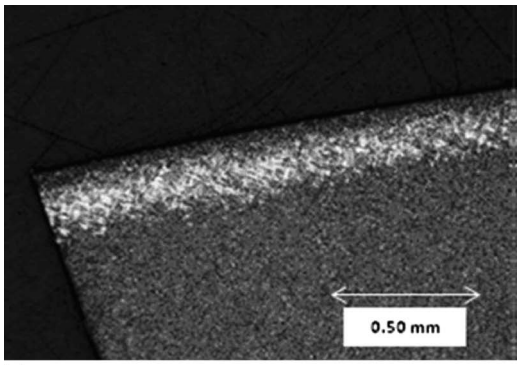

(*a*)

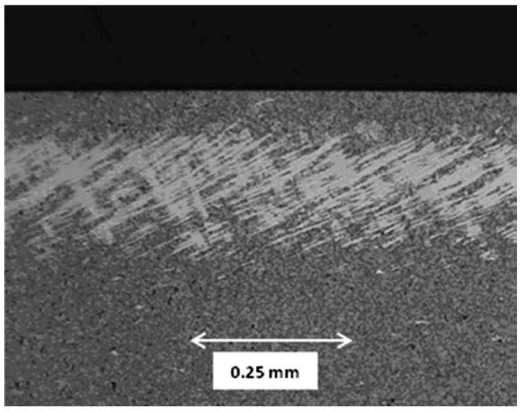

(*b*)

Fig. 8 Cross section of M50 Bearing 216 slightly past the spalled area showing slip bands: (*a*) circumferential cross section, and (*b*) circumferential cross section at higher magnification [79]

the RCF problem from a different viewpoint, by treating the material in the contact region as a nonhomogeneous microstructure consisting of randomly shaped, sized, and oriented structures that are sized to be the same as a grain in bearing material. This microlevel modeling is motivated by the fact that at some level, all physical materials are discontinuous. Commercially used bearing materials, including bearing steels and bearing grade ceramics, exhibit a granular microstructure [84] with average grain sizes of the order of $1-10$ μm. These materials have a nonhomogeneous microstructure at the micron level, where the grain boundaries can act as physical discontinuities in the system. In bearing contacts where the characteristic length scale is of the order of hundreds of microns, the microstructural length scale is no longer negligible. In these cases, it is reasonable to look at the material domain as a granular matrix. Better understanding of the microscopic mechanisms of failure can be obtained through such analyses where some of the microgeometric material features are included.

The proposed approaches offer several advantages over existing research models for RCF life. First, they are based on a nonhomogeneous description of the material. In this regard, they can easily incorporate the effects of material inclusions in bearing contacts. Second, unlike the crack propagation approaches adopted in literature where some initial crack geometry and location are assumed, the present approaches do not require the presence of initial cracks or flaws in the material domain. In fact, cracks can be naturally initiated under the contact loading and can continue to grow if the stress conditions permit. Third, instead of presuming a Weibull slope, the new approaches are capable of modeling the scatter in crack initiation and propagation lives and obtaining the Weibull slope as an output of simulations. Finally, the models have the potential to offer more insight into the physical mechanism of the failure process occurring during RCF.

5 Computational Models for Rolling Contact Fatigue

As mentioned earlier, Lundberg and Palmgren [34] applied the Weibull weakest link theory to formulate an empirical life formula (Eq. (1)) for bearing lives. The scatter in bearing lives was taken into account through the parameter e that represents the Weibull slope for experimentally observed bearing lives. As shown in Secs. 2 and 3, Ioannides and Harris [37], Zhou [53], Zaretsky [43], and Cheng and Cheng [57] proposed similar empirical models to Lundberg and Palmgren [33]. The underlying idea in the development of the empirical life models is a direct application of the Weibull strength theory without explicit incorporation of the material microstructural characteristics. In other words, it is assumed that the lives follow a Weibull distribution, rather than the resultant life distribution being an outcome of the inhomogeneous and random nature of the material microstructure. Raje et al. [85] presented a statistical model to estimate life scatter in rolling element bearings that took the material microstructure explicitly into account. Their modeling approach is based on a discrete rather than a continuous representation of the material in the bearing contact region [86,87]. The semi-infinite domain constituting the subsurface region in the bearing line contact is assumed to be formed by an assemblage of discrete, interacting, micro-elements, as shown in Fig. 9. These micro-elements are connected along their contacting sides through fibers to form compliant joints (Fig. 10(*a*)). Loads applied on the boundary of the domain are transferred to the internal elements through deformation of these joints. As shown in Fig. 10(*b*), each interelement joint comprises of both normal and tangential fiber sets, so that elements can overlap in

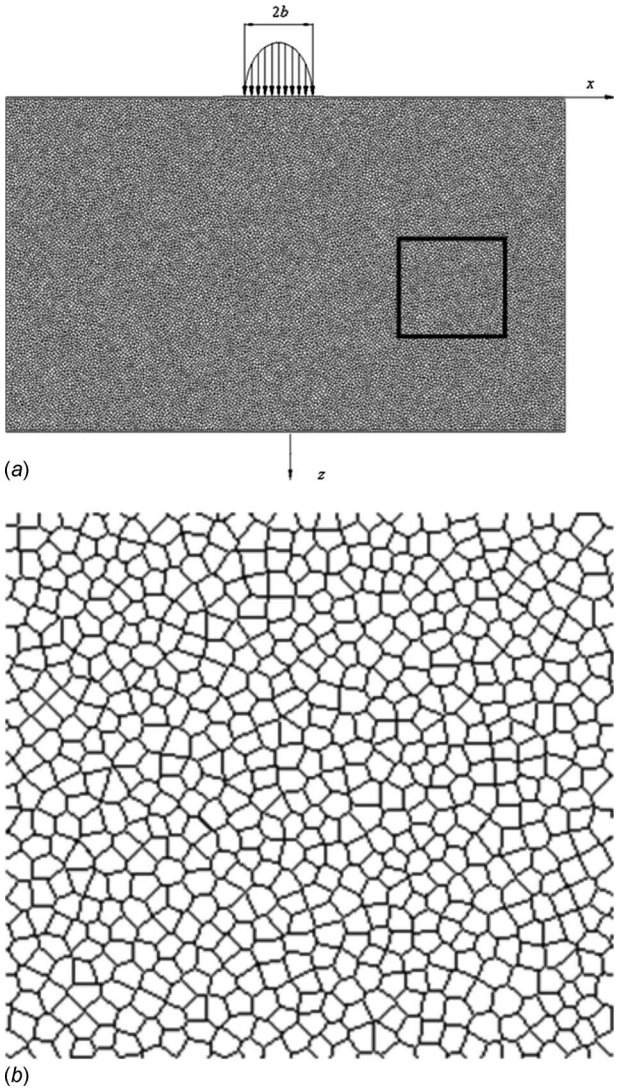

Fig. 9 (*a*) Discrete representation of the semi-infinite domain forming the bearing line contact; (*b*) zoomed view

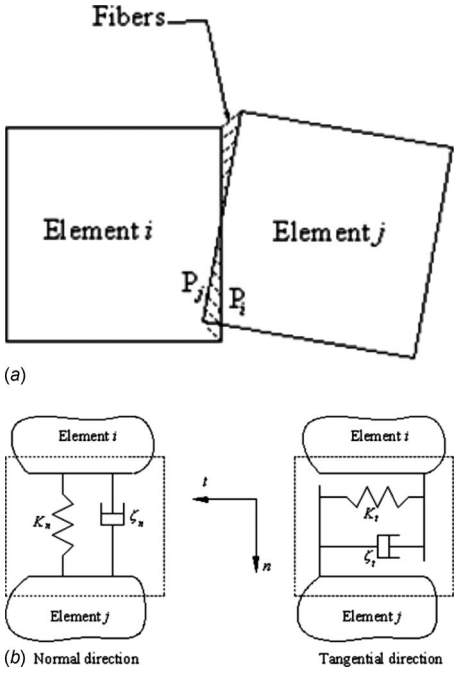

Fig. 10 (*a*) Interelement contact in the discrete model; (*b*) fiber model

the normal direction as well as slide relative to each other. Thus, both normal and shear tractions are transferred between elements. The fibers are assumed to be linear-elastic, and the fiber stiffnesses, namely, K_n in the normal direction and K_t in the tangential direction, are related to the macroscopic elastic properties E and ν [86]. By assigning unique fiber stiffnesses to each joint, the material domain can be made nonhomogeneous. Due to the interelement connectivity, the overall material domain behaves as a single, deformable body. The stress fields in such a discontinuous material domain are obtained through the solution of equations of motion for each element independently. Details of the solution scheme and the discrete element model used to obtain the stress field can be found in Ref. [86].

It is hypothesized that it is the variation in the magnitude and location of the critical stress quantity that leads to scatter in the bearing fatigue life. The model does not explicitly assume a Weibull distribution of fatigue lives. Rather, the life distribution is an outcome of numerical simulations performed using statistically generated material microstructures. The microstructures are generated using the process of Voronoi tessellation. Two sources of randomness in the material are considered: (1) the topological randomness due to geometric variability in the material microstructure and (2) material property randomness due to a statistical distribution of material properties spatially throughout the material. The fatigue life N is assumed to be related to the critical stress and the corresponding depth quantities by a relation of the form

$$N \sim \frac{z^r}{\tau^q} \tag{21}$$

However, an explicit Weibull life distribution is not assumed; i.e., the equation is independent of the Weibull slope e. Instead, the critical stress and depth quantities τ and z are assumed to be the variable parameters that lead to variability in life. This variation occurs due to randomness in the material microstructural characteristics. For convenience, the exponents q and r are assumed to be the same as the exponents c and h in the original Lundberg–Palmgren theory [33]. It is assumed that fatigue damage occurs along internal planes of weakness that are subjected to alternate shear stressing. Fatigue damage first starts along planes that experience the maximum range of alternating shear stress during the loading cycle. This is in accordance with several multiaxial fatigue criteria proposed in literature [25,27]. Figure 11 illustrates the effect of variable number of internal flaws on life distribution. It was found that lives are distributed according to a two-parameter Weibull distribution with Weibull slopes ranging from 1.29 to 3.36. Similarly, there is a reduction in the Weibull slope e with increasing number of flaws. Further, the results reach a limiting value beyond which there is no change in the Weibull slope with further increase in number of flaws, as observed in Fig. 12. The limiting value of e is found to be 1.29, which is close to the value of 1.125 used in the Lundberg–Palmgren theory [33].

Jalalahmadi and Sadeghi [88] proposed a new Voronoi finite element method (VFEM) using the Voronoi tessellation to simulate the material microstructure and its effects on rolling contact fatigue. In their model, a fatigue life criterion similar to Raje et al. [85] (Eq. (21)) was adopted, but instead of employing the discrete element method (DEM), they used the Voronoi finite element method as the numerical model to investigate the effects of material microstructure on rolling contact fatigue. Again, unlike the Lundberg–Palmgren theory [33] an explicit Weibull life distribution was not assumed, instead the critical stress and its depth were assumed to be the variable parameters, occurring because of the

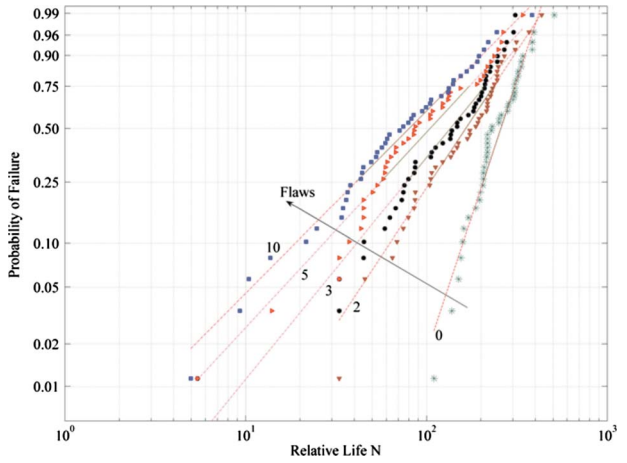

Fig. 11 Life distributions in the presence of variable number of flaws

random shape and size of grains in the material microstructure that lead to variability in the life. They considered both the maximum range of octahedral shear stress ($\Delta\tau_{xy}$) and the maximum unidirectional shear stress ($\tau_{\max}$) as the critical stress quantities. They studied the effects of material microstructure topology, nonuniform elastic properties, and initial flaws on rolling contact fatigue. The Weibull slopes of the fatigue lives calculated by their model agreed with the experimental works [89] and the analytical results [85]. They showed that considering material inhomogeneity using elastic modulus variation and initial flaws increased the average value of the critical stresses and changed the depths relative to the values obtained for the homogeneous domains. However, the average value and range of depths remain relatively the same for both homogeneous and inhomogeneous domains. According to their results, introducing both inhomogeneous material properties and initial cracks into the domains reduced the fatigue lives and increase their scatter. A general reference for the properties of Voronoi tessellation is given by Okabe and Boots [90] and a more mathematical one by Moller [91].

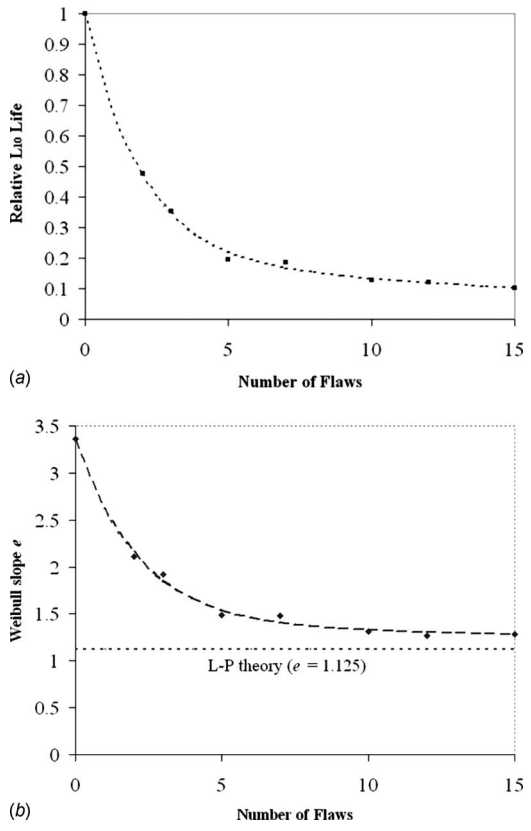

Fig. 12 Effect of internal flaws on (*a*) L_{10} life and (*b*) Weibull slope *e*

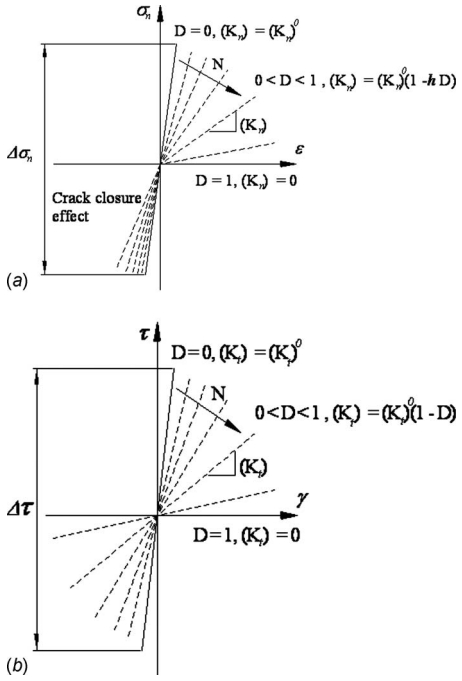

Fig. 13 Degradation of joint stiffnesses with damage accumulation: (*a*) normal direction and (*b*) tangential direction

The model presented in Ref. [85] was restricted to predicting only the life distributions and not the absolute lives. It was further improved upon in Ref. [92] by coupling it with a damage mechanics based fatigue model to explicitly take into account the gradual material degradation that occurs under rolling contact cycling. Damage was incorporated through an internal damage variable D and was implemented through degradation of the joint spring stiffnesses. Figure 13 shows the degradation of joint stiffnesses under cyclic loading. Damage evolution is assumed to occur according to an equation of the following form:

$$\frac{dD}{dN} = \left[\frac{\Delta\tau}{\sigma_r(1-D)}\right]^m \tag{22}$$

Here, $\Delta\tau$ is the shear stress range acting along the interelement joint. The parameters σ_r and m are material parameters that are determined from torsional fatigue tests according to the following equations:

$$m = B, \quad \sigma_r = 2\tau_f(B+1)^{1/B} \tag{23}$$

Here, B is the slope of the torsional S-N curve for the material and τ_f is known as the torsional fatigue strength coefficient, which is also determined from the torsional S-N curve. A microcrack was assumed to be initiated at an interelement joint when the accumulated damage in it equaled unity ($D=1$). The process of spalling was modeled through growth of damaged zones in the material. Final failure is defined when a crack reaches the surface. Figure 14 shows a sample spall formation process. Spall formation is manifested through several distinct cracks rather than a single crack as assumed in models based on fracture mechanics [49,93]. This observation has been made experimentally by several researchers using metallographic examinations of spalled sections of contacting elements [14,46,47,81].

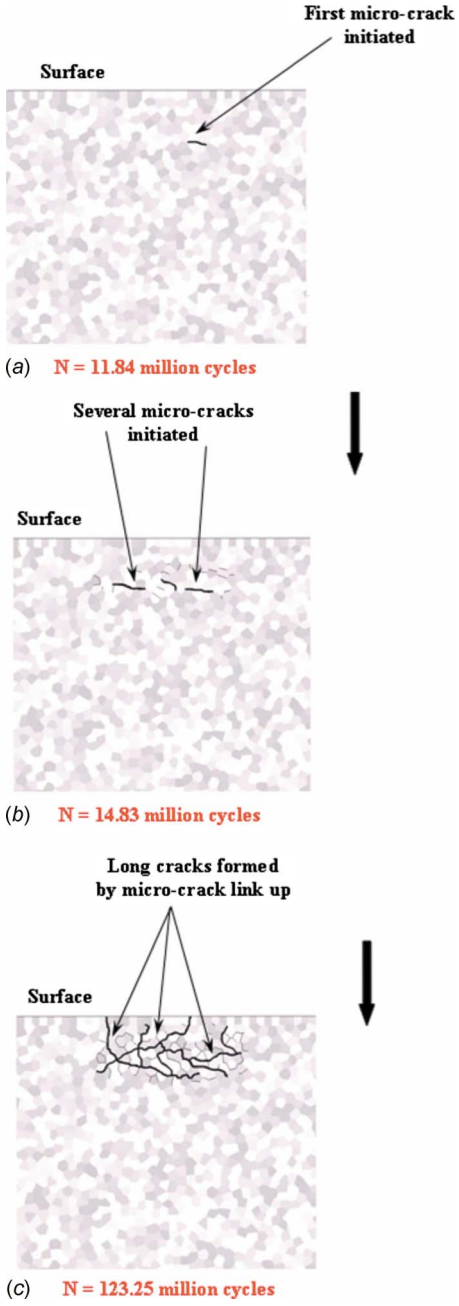

Fig. 14 Formation of subsurface initiated spall through microcrack initiation and coalescence: (*a*) first microcrack initiated (11.84×10^6 cycles), (*b*) multiple microcracks initiated (14.83×10^6 cycles), and (*c*) multiple crack coalescence and spall formation (123.25×10^6 cycles)

Figure 15 depicts the variation of the initiation and propagation lives for multiple material domains. The initiation life is defined as the number of cycles elapsed before the first microcrack appears. The subsequent number of cycles before a surface breaking crack forms constitutes the propagation life. It is observed that the initiation phase of fatigue life is a small fraction of the total life, with the average initiation life for the 40 domains being about 20% of their total life. In relation to the total fatigue lives, the initiation lives do not show much scatter between domains and the overall scatter in the total lives is primarily governed by the scatter in propagation lives. The Weibull slopes (e) for the initiation and total lives using a two-parameter Weibull fit are 11.75 and 1.85, respectively. However, the total lives are found to follow a

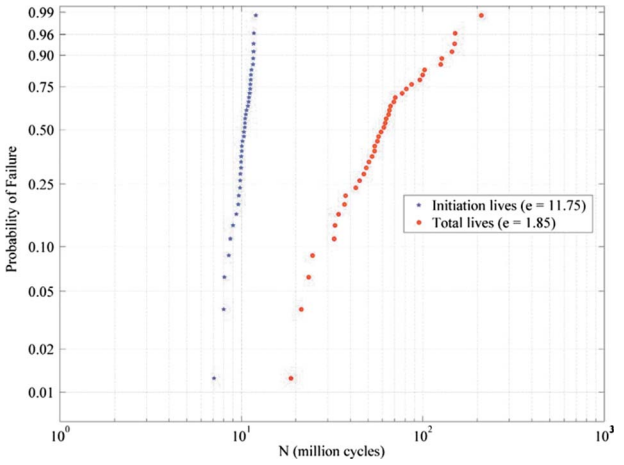

Fig. 15 Weibull life plots for different material domains with constant material properties

three-parameter Weibull distribution more closely. Figure 16 shows the stress-life curve obtained from model simulations. Here, the L_{10} lives are plotted against the contact pressure p_{max}. Table 3 shows the corresponding stress-life exponents obtained from the model and compares them with those obtained from other models in literature.

Recently, Raje and Sadeghi [94] developed a statistical life equation for subsurface initiated spalling of bearing elements based on the life distributions and the stress-life results obtained through their simulations. They showed that the spalling lives follow a three-parameter Weibull distribution closely. Using the general equation for the three-parameter Weibull distribution and their simulation results, they expressed the spalling life N as

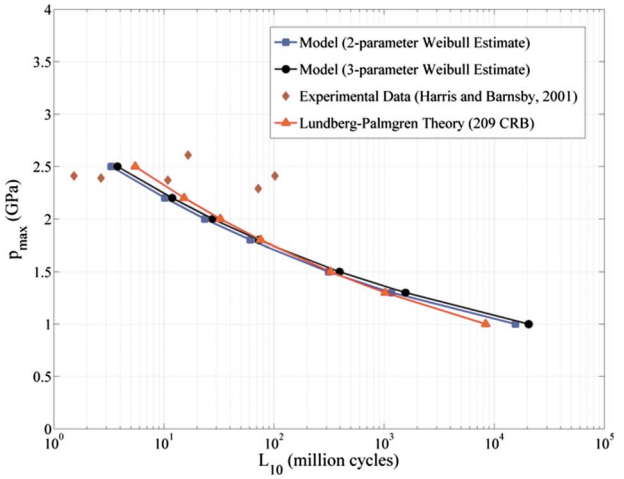

Fig. 16 Variation of L_{10} life with contact pressure

Table 3 Comparison of stress-life exponents for line contacts

Source	Stress-life exponent
Raje et al. [92] (two-parameter Weibull estimate)	8.93
Raje et al. [92] (three-parameter Weibull estimate)	9.38
Lundberg and Palmgren [33]	8
Poplawski et al. [95]	9.9

Table 4 Comparison of life equations

Source	Life equation
Raje and Sadeghi [94]	$N=\frac{39354}{p_{\max}^{8.74}}\left[\ln\left(\frac{1}{S}\right)\right]^{0.58}$
Lundberg–Palmgren theory [33] ($c=10.33$, $h=2.33$, $e=1.125$, $M_1=4.056\times10^{-6}$)	$N=\frac{62037}{p_{\max}^{8}}\left[\ln\left(\frac{1}{S}\right)\right]^{0.88}$

$$\ln\left(\frac{1}{S}\right)=\frac{1}{B_1^e}\cdot p_{\max}^{e(f-d)}\cdot N^e\cdot\left\{p_{\max}^d-\frac{A_1}{N}\right\}^e \tag{24}$$

where $p_{\max}$ is maximum Hertzian contact pressure, S is probability of survival, e is Weibull parameter, d is power law exponent for Weibull minimum life parameter, f is power law exponent for Weibull scale parameter, A_1 is power law constant for Weibull minimum life parameter, and B_1 is power law constant for Weibull scale parameter. Moreover, they rearranged the Lundberg–Palmgren equation (Eq. (1)) [33] in terms of the contact pressure as

$$\ln\left(\frac{1}{S}\right)=M_1\cdot p_{\max}^{c-h+1}\cdot N^e \tag{25}$$

From Eqs. (24) and (25), it can be observed that their life equation is similar in form to the original Lundberg–Palmgren equation [33], with a modification term. In the absence of a minimum life (i.e., using a two-parameter Weibull fit), Eq. (24) reduces to a form similar to Eq. (25). Table 4 lists the two equations using two-parameter Weibull values obtained from their simulations and the original values used by Lundberg and Palmgren [33]. Figure 17 depicts the comparison between these two life equations using a probability of survival equal to 0.9. As observed there is a good agreement between the two life models.

6 Summary

RCF is the most unavoidable mode of failure of ball and rolling element bearings. There are two most dominant mechanisms for RCF, i.e., the subsurface originated spalling and surface originated pitting. In this paper, a review of the most acceptable empirical and research models, existing in literature, developed for investigating the rolling contact fatigue caused by subsurface originated spalling was provided. Tables 1 and 2 provide a concise summary of the empirical and research models, respectively. Though the empirical models are practical life prediction tools, they do not take the material microstructure explicitly into account. The underlying idea in the development of the empirical life models is a direct application of the Weibull strength theory without explicit incorporation of the material microstructural characteristics. In other words, it is assumed that the lives follow a Weibull distribution, rather than the resultant life distribution being an outcome of the inhomogeneous and random nature of the material microstructure. On the other hand, the research models are based on a homogeneous description of the material in the contact region to estimate the contact fatigue life. However, subsurface initiated spalling, which is the classical mode of failure in rolling element bearings that operate under conditions of EHL, is significantly influenced by the material microstructure, which is inherently inhomogeneous due to the presence of defects and nonuniform distribution of material properties. As a result of these inhomogeneous material microstructures, spalling lives of a seemingly identical batch of bearings operating under identical load, speed, lubrication, and environmental conditions show a significant degree of scatter.

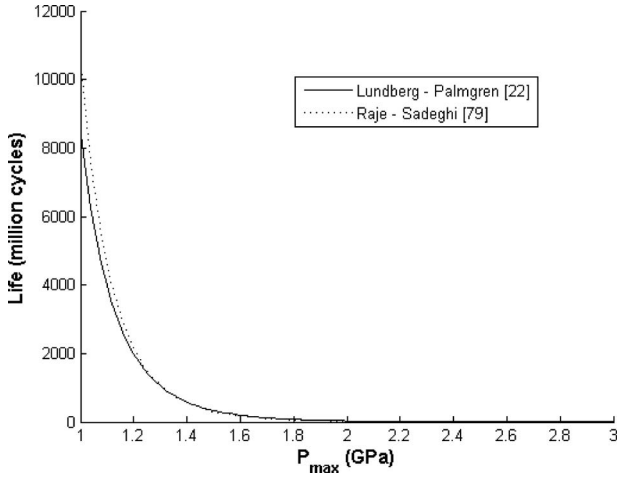

Fig. 17 The comparison between two life equations using a probability of survival equal to 0.9

In view of the limitations of the current state of bearing life modeling, some research models recently proposed by the authors, in order to predict the fatigue lives of the rolling element bearings, were reviewed. The new approaches, including DEM [85] and VFEM [88], investigate the RCF problem from a different viewpoint, by treating the material in the contact region as a nonhomogeneous microstructure consisting of randomly shaped, sized, and oriented grains. Contrary to the Lundberg–Palmgren theory [33], the developed models hypothesized that it is the variation in the magnitude and location of the critical stress quantity that leads to scatter in the bearing fatigue life. The models do not explicitly assume a Weibull distribution of fatigue lives. Rather, the life distribution is an outcome of numerical simulations performed using statistically generated material microstructures. The microstructures are generated using the process of Voronoi tessellation. Also, the DEM model was further extended [92] by coupling it with a damage mechanics based fatigue model to explicitly take into account the gradual material degradation that occurs under rolling contact cycling. As a result, not only the life distributions, but also the absolute lives of bearings could be predicted. It was observed that the Weibull slopes for the fatigue lives and the fatigue crack initiation depths, obtained using the models, agree with the experimental works [82,89]. Moreover, based on the statistical distribution of spalling lives and the resultant stress-life results, a new life equation was proposed [94], which is similar in structure to the original Lundberg–Palmgren equation [33] with a modification term.

References

[1] Voskamp, A. P., Osterlund, R., Becker, P. C., and Vingsbo, O., 1980, "Gradual Changes in Residual Stress and Microstructure During Contact Fatigue in Ball Bearings," Met. Technol. (London), **7**, pp. 14–21.

[2] Osterlund, R., and Vingsbo, O., 1980, "Phase Changes in Fatigued Ball Bearings," Metall. Trans. A, **11**, pp. 701–707.

[3] Voskamp, A. P., 1985, "Material Response to Rolling Contact Loading," ASME J. Tribol., **107**, pp. 359–366.

[4] Voskamp, A. P., 1998, "Fatigue and Material Response in Rolling Contact," *Bearing Steels: Into the 20th Century*, ASTM STP No. 1328, ASTM Special Technical Publication, West Conshohocken, PA, pp. 152–166.

[5] Voskamp, A. P., and Mittemeijer, E. J., 1997, "The Effect of the Changing Microstructure on the Fatigue Behavior During Cyclic Rolling Contact Loading," Z. Metallkd., **88**, pp. 310–319.

[6] Hahn, G. T., Bhargava, V., and Chen, Q., 1990, "The Cyclic Stress-Strain Properties, Hysteresis Loop Shape, and Kinematic Hardening of Two High-Strength Bearing Steels," Metall. Trans. A, **21**, pp. 653–665.

[7] Voskamp, A. P., 2002, "Microstructural Stability and Bearing Performance," *Bearing Steel Technology*, ASTM STP No. 1419, ASTM Special Technical Publication, West Conshohocken, PA, pp. 443–456.

[8] Voskamp, A. P., Nierlich, W., and Hengerer, F., 1997, "X-Ray Diffraction Provides Answers to Bearing Failures," SKF Evolution, **4**, pp. 25–31.

[9] Voskamp, A. P., and Mittemeijer, E. J., 1997, "State of Residual Stress Induced by Cyclic Rolling Contact Loading," Mater. Sci. Technol., **13**, pp. 431–438.

[10] Turteltaub, S., and Suiker, A. S. J., 2005, "Transformation-Induced Plasticity in Ferrous Alloys," J. Mech. Phys. Solids, **53**, pp. 1747–1788.

[11] Voskamp, A. P., and Mittemeijer, E. J., 1996, "Crystallographic Preferred Ori-

entation Induced by Cyclic Rolling Contact Loading," Metall. Mater. Trans. A, **27**, pp. 3445–3465.
[12] Littmann, W. E., and Widner, R. L., 1966, "Propagation of Contact Fatigue From Surface and Sub-Surface Origins," ASME J. Basic Eng., **88**, pp. 624–636.
[13] Littmann, W. E., 1969, "The Mechanism of Contact Fatigue," NASA, Special Report No. SP-237.
[14] Lou, B., Han, L., Lu, Z., Liu, S., and Shen, F., 1990, "The Rolling Contact Fatigue Behaviors in Carburized and Hardened Steel," *Fatigue 90: Proceedings of the Fourth International Conference on Fatigue and Fatigue Thresholds*, Honolulu, HI, H. Kitagawa and T. Tanaka, eds., pp. 627–632.
[15] Bower, A. F., 1988, "The Influence of Crack Face Friction and Trapped Fluid on Surface Initiated Rolling Contact Fatigue Cracks," ASME J. Tribol., **110**, pp. 704–711.
[16] Nelias, D., Dumont, M. L., Champiot, F., Vincent, A., Girodin, D., Fougeres, R., and Flamand, L., 1999, "Role of Inclusions, Surface Roughness and Operating Conditions on Rolling Contact Fatigue," ASME J. Tribol., **121**(2), pp. 240–251.
[17] Hertz, H., 1882, "On the Contact of Elastic Solids," J. Reine Angew. Math., **92**, pp. 156–171.
[18] McEwen, E., 1949, "Stresses in Elastic Cylinders in Contact Along a Generatrix," Philos. Mag., **40**, pp. 454–459.
[19] Poritsky, H., 1950, "Stresses and Deflections of Cylindrical Bodies in Contact," ASME J. Appl. Mech., **17**, pp. 191–201.
[20] Smith, J. O., and Liu, C. K., 1953, "Stresses Due to Tangential and Normal Loads on an Elastic Solid," ASME J. Appl. Mech., **20**, pp. 157–166.
[21] Sackfield, A., and Hills, D. A., 1983, "Some Useful Results in the Classical Hertz Contact Problem," J. Strain Anal., **18**, pp. 101–105.
[22] Sackfield, A., and Hills, D. A., 1983, "Some Useful Results in the Tangentially Loaded Hertz Contact Problem," J. Strain Anal., **18**, pp. 107–110.
[23] Sackfield, A., and Hills, D. A., 1983, "A Note on the Hertz Contact Problem: Correlation of Standard Formulae," J. Strain Anal., **18**, pp. 195–197.
[24] Johnson, K. L., 1985, *Contact Mechanics*, Cambridge University, Cambridge.
[25] McDiarmid, D. L., 1991, "A General Criterion for High Cycle Multi-Axial Fatigue Failure," Fatigue Fract. Eng. Mater. Struct., **14**, pp. 429–453.
[26] McDiarmid, D. L., 1994, "A Shear Stress Based Critical-Plane Criterion of Multiaxial Fatigue Failure for Design and Life Prediction," Fatigue Fract. Eng. Mater. Struct., **17**, pp. 1475–1484.
[27] Susmel, L., and Lazzarin, P., 2002, "A Bi-Parametric Wohler Curve for High Cycle Multi-Axial Fatigue Assessment," Fatigue Fract. Eng. Mater. Struct., **25**(1), pp. 63–78.
[28] Papadopoulos, I. V., 1995, "A High-Cycle Fatigue Criterion Applied in Biaxial and Triaxial Out-of-Phase Stress Conditions," Fatigue Fract. Eng. Mater. Struct., **18**, pp. 79–91.
[29] Brown, M. W., and Miller, K. J., 1973, "A Theory for Fatigue Failure Under Multiaxial Stress-Strain Conditions," Proc. Inst. Mech. Eng., **187**, pp. 745–755.
[30] Socie, D. F., and Shield, T. W., 1984, "Mean Stress Effects in Biaxial Fatigue of Inconel 718," ASME J. Eng. Mater. Technol., **106**, pp. 227–232.
[31] Socie, D. F., 1987, "Multiaxial Fatigue Damage Models," ASME J. Eng. Mater. Technol., **109**, pp. 292–298.
[32] Palmgren, A., 1945, *Ball and Roller Bearing Engineering*, SKF Industries, Philadelphia, PA.
[33] Lundberg, G., and Palmgren, A., 1947, "Dynamic Capacity of Rolling Bearings," Acta Polytech. Scand., Mech. Eng. Ser., **1**(3), pp. 1–52.
[34] Lundberg, G., and Palmgren, A., 1952, "Dynamic Capacity of Roller Bearings," Acta Polytech. Scand., Mech. Eng. Ser., **2**(4), pp. 96–127.
[35] ISO, 1989, "Rolling Bearings—Dynamic Load Ratings and Rating Life," Draft International Standard ISO/DIS 281, ISO, Geneva, Switzerland.
[36] Chiu, Y. P., Tallian, T. E., and McCool, J. I., 1971, "An Engineering Model of Spalling Fatigue Failure in Rolling Contact—The Subsurface Model," Wear, **17**, pp. 433–446.
[37] Ioannides, E., and Harris, T. A., 1985, "A New Fatigue Life Model for Rolling Bearings," ASME J. Tribol., **107**, pp. 367–378.
[38] Ioannides, E., Bergling, G., and Gabelli, A., 1999, "An Analytical Formulation for the Life of Rolling Bearings," Acta Polytech. Scand., Mech. Eng. Ser., **137**, pp. 58–60.
[39] Harris, T. A., and Barnsby, R. M., 2001, "Life Ratings for Ball and Roller Bearings," Proc. Inst. Mech. Eng., Part J: J. Eng. Tribol., **215**, pp. 577–595.
[40] Schlicht, H., Schreiber, E., and Zwirlein, O., 1986, "Fatigue and Failure Mechanism of Bearings," I Mech E Conf. Publ., **1**, pp. 85–90.
[41] Tallian, T. E., 1992, "Simplified Contact Fatigue Life Prediction Model—Part I: Review of Published Models," ASME J. Tribol., **114**, pp. 207–213.
[42] Tallian, T. E., 1992, "Simplified Contact Fatigue Life Prediction Model—Part II: New Model," ASME J. Tribol., **114**, pp. 214–222.
[43] Zaretsky, E. V., 1994, "Design for Life, Plan for Death," Mach. Des., **66**(15), pp. 55–59.
[44] Harris, T. A., and McCool, J., 1996, "On the Accuracy of Rolling Bearing Fatigue Life Prediction," ASME J. Tribol., **118**, pp. 297–310.
[45] Kudish, I. I., and Burris, K. W., 2000, "Modern State of Experimentation and Modeling in Contact Fatigue Phenomenon: Part II—Analysis of the Existing Statistical Mathematical Models of Bearing and Gear Fatigue Life. New Statistical Model of Contact Fatigue," Tribol. Trans., **43**(2), pp. 293–301.
[46] Shao, E., Huang, X., Wang, C., Zhu, Y., and Chen, Q., 1987, "A Method of Detecting Rolling Contact Crack Initiation and the Establishment of Crack Propagation Curves," Tribol. Trans., **31**(1), pp. 6–11.
[47] Leng, X., Chen, Q., and Shao, E., 1988, "Initiation and Propagation of Case Crushing Cracks in Rolling Contact Fatigue," Wear, **122**, pp. 33–43.
[48] Otsuka, A., Sugawara, H., and Shomura, M., 1996, "A Test Method for Mode II Fatigue Crack Growth Relating to a Model for Rolling Contact Fatigue," Fatigue Fract. Eng. Mater. Struct., **19**(10), pp. 1265–1275.
[49] Miyashita, Y., Yoshimura, Y., Xu, J.-Q., Horikoshi, M., and Mutoh, Y., 2003, "Subsurface Crack Propagation in Rolling Contact Fatigue of Sintered Alloy," JSME Int. J., Ser. A, **46**(3), pp. 341–347.
[50] Shimizu, S., 2002, "Fatigue Limit Concept and Life Prediction Model for Rolling Contact Machine Elements," Tribol. Trans., **45**(1), pp. 39–46.
[51] Kotzalas, M. N., 2005, "Statistical Distribution of Tapered Roller Bearing Fatigue Lives at High Levels of Reliability," ASME J. Tribol., **127**(4), pp. 865–870.
[52] Keer, L. M., and Bryant, M. D., 1983, "A Pitting Model for Rolling Contact Fatigue," ASME J. Lubr. Technol., **105**, pp. 198–205.
[53] Zhou, R. S., Cheng, H. S., and Mura, T., 1989, "Micropitting in Rolling and Sliding Contact Under Mixed Lubrication," ASME J. Tribol., **111**, pp. 605–613.
[54] Zhou, R. S., 1993, "Surface Topography and Fatigue Life of Rolling Contact Bearings," Tribol. Trans., **36**, pp. 329–340.
[55] Bhargava, V., Hahn, G. T., and Rubin, C. A., 1990, "Rolling Contact Deformation, Etching Effects and Failure of High Strength Steels," Metall. Trans. A, **21**, pp. 1921–1931.
[56] Cheng, W., Cheng, H. S., Mura, T., and Keer, L. M., 1994, "Micromechanics Modeling of Crack Initiation Under Contact Fatigue," ASME J. Tribol., **116**, pp. 2–8.
[57] Cheng, W., and Cheng, H. S., 1995, "Semi-Analytical Modeling of Crack Initiation Dominant Contact Fatigue for Roller Bearings," Proceedings of the 1995 Joint ASME/STLE Tribology Conference, Orlando, FL.
[58] Vincent, A., Lormand, G., Lamagnere, P., Gosset, L., Girodin, D., Dudragne, G., and Fougeres, R., 1998, "From White Etching Areas Formed Around Inclusions to Crack Nucleation in Bearing Steels Under Rolling Contact," *Bearing Steels: Into the 21st Century*, ASTM STP No. 1327, J. Hoo and W. Green, eds., ASTM Special Technical Publication, West Conshohocken, PA, pp. 109–123.
[59] Xu, G., and Sadeghi, F., 1996, "Spall Initiation and Propagation Due to Debris Denting," Wear, **201**, pp. 106–116.
[60] Lormand, G., Meynaud, G., Vincent, A., Baudry, G., Girodin, D., and Dudragne, G., 1998, "From Cleanliness to Rolling Fatigue Life of Bearings—A New Approach," *Bearing Steels: Into the 21st Century*, ASTM STP No. 1327, J. Hoo and W. Green, eds., ASTM Special Technical Publication, West Conshohocken, PA, pp. 55–69.
[61] Ashby, M. F., and Hallam, S. D., 1986, "The Fracture of Brittle Solids Containing Small Cracks Under Compressive Stress States," Acta Mater., **34**, pp. 497–510.
[62] Melander, A., 1997, "A Finite Element Study of Short Cracks With Different Inclusion Types Under Rolling Contact Fatigue Load," Int. J. Fatigue, **19**(1), pp. 13–24.
[63] Lormand, G., Piot, D., Vincent, A., Baudry, G., Daguier, P., Girodin, G., and Dudragne, G., 2002, "Application of a New Physically Based Model to Determine the Influence of Inclusion Population and Loading Conditions on the Distribution of Bearing Lives," *Proceedings of the ASTM Symposium Bearing Steel Technology*, ASTM Publication No. STP1419, pp. 493–508.
[64] Girodin, D., Dudragne, G., Courbon, J., and Vincent, A., 2006, "Statistical Analysis of Nonmetallic Inclusions for the Estimation of Rolling Contact Fatigue Range and Quality Control of Bearing Steel," J. ASTM Int., **3**, pp. 1–16.
[65] Harris, T. A., and Yu, W. K., 1999, "Lundberg-Palmgren Fatigue Theory: Considerations of Failure Stress and Stressed Volume," ASME J. Tribol., **121**, pp. 85–89.
[66] Jiang, Y., and Sehitoglu, H., 1999, "A Model for Rolling Contact Failure," Wear, **224**, pp. 38–49.
[67] Sehitoglu, H., and Jiang, Y., 1992, "Fatigue and Stress Analyses of Rolling Contact," College of Engineering, University of Illinois at Urbana-Champaign, Technical Report No. 161.
[68] Ringsberg, J. W., 2001, "Life Prediction of Rolling Contact Fatigue Crack Initiation," Int. J. Fatigue, **23**(7), pp. 575–586.
[69] Liu, Y., Stratman, B., and Mahadevan, S., 2006, "Fatigue Crack Initiation Life Prediction of Railroad Wheels," Int. J. Fatigue, **28**, pp. 747–756.
[70] Liu, Y., and Mahadevan, S., 2007, "A Unified Multiaxial Fatigue Damage Model for Isotropic and Anisotropic Materials," Int. J. Fatigue, **29**, pp. 347–359.
[71] Styri, H., 1951, "Fatigue Strength of Ball Bearing Races and Heat-Treated 52100 Steel Specimens," Proc. of the American Society for Testing and Materials, ASTM Special Technical Publication, Philadelphia, PA, No. 51, pp. 682–700.
[72] Nishioka, K., 1957, "On the Effect of Inclusion Upon the Fatigue Strength," J. Soc. Mater. Sci. Jpn., **6**, pp. 382–385.
[73] Murakami, Y., Kodama, S., and Konuma, S., 1989, "Quantitative Evaluation of Effects of Non-Metallic Inclusions on Fatigue Strength of High Strength Steels. I: Basic Fatigue Mechanism and Evaluation of Correlation Between the Fatigue Fracture Stress and the Size and Location of Non-Metallic Inclusions," Int. J. Fatigue, **11**(5), pp. 291–298.
[74] Bohmer, H. J., 1993, "Rolling Contact Fatigue," *Research—A Basis for Products of the Future*, Publication No. WL40205EA, FAG Kugelfischer Georg Schafer KGaA, Schweinfurt, Germany, pp. 37–45.
[75] Bohmer, H. J., 1993, "A New Approach to Determine the Effect of Nonmetallic Inclusions on Material Behavior in Rolling Contact," *Creative Use of Bearing Steels*, ASTM STP No. 1195, J. J. C. Hoo, ed., American Society for

Testing and Materials, Philadelphia, PA, pp. 211–221.
[76] Martin, J. A., Borgese, S. F., and Eberhardt, A. D., 1966, "Microstructural Alterations of Rolling-Bearing Steel Undergoing Cyclic Stressing," ASME J. Basic Eng., **88**, pp. 555–567.
[77] O'Brien, J. L., and King, A. H., 1966, "Electron Microscopy of Stress-Induced Structural Alterations Near Inclusions in Bearing Steels," ASME J. Basic Eng., **88**, pp. 568–572.
[78] Schlicht, H., Schreiber, E., and Zwirlein, O., 1988, "Effects of Material Properties on Bearing Steel Fatigue Strength," *Effects of Steel Manufacturing Processes on the Quality of Bearing Steels*, ASTM STP No. 987, J. C. C. Hoo, ed., ASTM Special Technical Pubication, Philadelphia, PA, pp. 81–101.
[79] Forster, N., Ogden, W. P., and Trivedi, H., 2008, "Rolling Contact Fatigue Life and Spall Propagation of AISI M50, M50NiL, and ASI 52100, Part III: Metallurgical Investigation," STLE Tribol. Trans., in press.
[80] Zaretsky, E. V., Parker, R. J., and Anderson, W. J., 1969, "A Study of Residual Stress Induced During Rolling," ASME J. Lubr. Technol., **91**, pp. 314–319.
[81] Chen, L., Chen, Q., and Shao, E., 1989, "Study on Initiation and Propagation Angles of Sub-Surface Cracks in GCr15 Bearing Steel Under Rolling Contact," Wear, **133**, pp. 205–218.
[82] Chen, Q., Shao, E., Zhao, D., Guo, J., and Fan, Z., 1991, "Measurement of the Critical Size of Inclusions Initiating Contact Fatigue Cracks and Its Application in Bearing Steel," Wear, **147**, pp. 285–294.
[83] Yoshioka, T., 1993, "Detection of Rolling Contact Subsurface Fatigue Cracks Using Acoustic Emission Technique," Lubr. Eng., **49**, pp. 303–308.
[84] Liu, M., and Sia, N., 1999, "Microstructure of Bearing Grade Silicon Nitride," J. Mater. Res., **14**(12), pp. 4621–4629.
[85] Raje, N. N., Sadeghi, F., Rateick, R. G., Jr., and Hoeprich, M. R., 2008, "A Numerical Model for Life Scatter in Rolling Element Bearings," ASME J. Tribol., **130**(1), p. 011011.
[86] Raje, N. N., Sadeghi, F., and Rateick, R. G., Jr., 2007, "A Discrete Element Approach to Evaluate Stresses Due to Line Loading on an Elastic Half-Space," Comput. Mech., **40**(3), pp. 513–529.
[87] Raje, N. N., Sadeghi, F., Rateick, R. G., Jr., and Hoeprich, M. R., 2007, "Evaluation of Stresses Around Inclusions in Hertzian Contacts Using the Discrete Element Method," ASME J. Tribol., **129**(2), pp. 283–291.
[88] Jalalahmadi, B., and Sadeghi, F., 2009, "A Voronoi Finite Element Study of Fatigue Life Scatter in Rolling Contacts," ASME J. Tribol., **131**, p. 022203.
[89] Harris, T. A., 2001, *Rolling Bearing Analysis*, Wiley, New York, p. 696.
[90] Okabe, A., and Boots, B., 1992, *Spatial Tessellations: Concepts and Applications of Voronoi Diagrams*, Wiley, New York.
[91] Moller, J., 1994, *Lectures Notes on Random Voronoi Tessellations*, Springer, Berlin.
[92] Raje, N. N., Sadeghi, F., and Rateick, R. G., Jr., 2008, "A Statistical Damage Mechanics Model for Subsurface Initiated Spalling in Rolling Contacts," ASME J. Tribol., **130**(4), p. 042201.
[93] Fajdiga, G., Glodez, S., and Kramar, J., 2007, "Pitting Formation Due to Surface and Sub-Surface Initiated Fatigue Crack Growth in Contacting Mechanical Elements," Wear, **262**, pp. 1217–1224.
[94] Raje, N. N., and Sadeghi, F., 2008, "Statistical Numerical Modeling of Sub-Surface Initiated Spalling in Bearing Contacts," Proc. Inst. Mech. Eng., Part J: J. Eng. Tribol., to be published.
[95] Poplawski, J. V., Peters, S. M., and Zaretsky, E. V., 2001, "Effect of Roller Profile on Cylindrical Roller Bearing Life Predication—Part I: Comparison of Bearing Life Theories," Tribol. Trans., **44**(3), pp. 339–350.